

Rapid report

Casting light on xylem vulnerability in an herbaceous species reveals a lack of segmentation

Author for correspondence:

Timothy J. Brodribb

Tel: +61 (0) 3 6226 1707

Email: Timothy.brodribb@utas.edu.au

Received: 23 November 2016

Accepted: 22 December 2016

Robert P. Skelton¹, Timothy J. Brodribb¹ and Brendan Choat²¹School of Biological Sciences, University of Tasmania, Private Bag 55, Hobart, TAS 7001, Australia; ²Hawkesbury Institute for the Environment, Western Sydney University, Richmond, NSW 2753, AustraliaNew Phytologist (2017) 214: 561–569
doi: 10.1111/nph.14450**Key words:** embolism, hydraulic conductance, optical vulnerability, *Solanum lycopersicum* (tomato), tomato, X-ray micro-computed tomography (microCT), xylem cavitation.

Summary

- Finding thresholds at which loss of plant functionality occurs during drought is critical for predicting future crop productivity and survival. Xylem resistance to embolism has been suggested as a key trait associated with water-stress tolerance. Although a substantial literature exists describing the vulnerability of woody stems to embolism, leaves and roots of herbaceous species remain under-represented. Also, little is known about vulnerability to embolism at a whole-plant scale or propagation of embolism within plants.
- New techniques to view the process of embolism formation provide opportunities to resolve long-standing questions. Here, we used multiple visual techniques, including X-ray micro-computed tomography and the optical vulnerability method, to investigate the spread of embolism within intact stems, leaves and roots of *Solanum lycopersicum* (common tomato).
- We found that roots, stems and leaves of tomato plants all exhibited similar vulnerability to embolism, suggesting that embolism rapidly propagates among tissues. Although we found scarce evidence for differentiation of xylem vulnerability among tissues at the scale of the whole plant, within a leaf the midrib embolized at higher water potentials than lower order veins.
- Substantial overlap between the onset of cavitation and incipient leaf damage suggests that cavitation represents a substantial damage to plants, but the point of lethal cavitation in this herbaceous species remains uncertain.

Introduction

Establishing robust determinants and thresholds of plant sensitivity to stress is crucial for assessing future productivity and survival (Challinor *et al.*, 2009). In this context, the ability of xylem to resist cavitation appears to be a key plant trait, able to predict plant distribution (Brodribb & Hill, 1999; Choat *et al.*, 2012; Brodribb *et al.*, 2014) and the timing of plant death during water stress (Brodribb & Cochard, 2009; Urli *et al.*, 2013). Water in a plants' xylem is transported under tension, which increases with higher rates of water loss or drying soil (Tyree & Sperry, 1989). At some critical water potential, termed the air-entry potential (P_c), tension in the water column exceeds the plants' ability to withstand air entry and air emboli form in xylem conduits (Zimmermann, 1983; Tyree & Sperry, 1988; Brodersen *et al.*, 2013). Emboli cause reductions in xylem hydraulic conductivity (k_{xylem}), hindering the ability of a plant to transport water. Parameters obtained from xylem

vulnerability curves (VCs) for a species – the relationship between k_{xylem} and xylem water potential – potentially provide quantitative indices for mortality thresholds within a species (Brodribb & Cochard, 2009; Choat *et al.*, 2012; Choat, 2013; Ogasa *et al.*, 2013; Urli *et al.*, 2013). For example, the threshold of drought mortality is closely associated with the water potential inducing 50% loss of stem k_{xylem} (P_{50}) in conifers (Brodribb & Cochard, 2009) and 88% loss of stem k_{xylem} (P_{88}) in angiosperms (Urli *et al.*, 2013).

Technical limitations in measuring embolism, particularly in leaves and softer tissues, have led to a situation where our understanding of species vulnerability to embolism is biased towards the stem and there is scarce information regarding the spatial and temporal propagation of embolism within a whole plant. This gap in our knowledge is problematic considering that the few studies examining multiple tissues have suggested considerable variation in vulnerability between stems and leaves (Tyree &

Ewers, 1991; Tyree *et al.*, 1991, 1993; Cochard *et al.*, 1992; Johnson *et al.*, 2011; Bucci *et al.*, 2012; Jinagool *et al.*, 2015; McCulloh *et al.*, 2015) or stems and roots (Alder *et al.*, 1996; Sperry & Ikeda, 1997; Kavanagh *et al.*, 1999; Froux *et al.*, 2004). Indeed, it has long been accepted that a gradient in vulnerability may exist within plants. This hydraulic segmentation hypothesis (HSH) states that more distal, less energy-intensive/expensive tissues, such as leaves, should be more susceptible to embolism than larger, more costly/valuable tissues, such as stems (Zimmermann, 1978; Tyree & Ewers, 1991). Support for the HSH has come from woody angiosperms and conifers (Alder *et al.*, 1996; Sperry & Ikeda, 1997; Choat *et al.*, 2005).

Recent technological and methodological advances allow us to assess vulnerability to embolism in all plant tissues using intact plants. These new techniques include, X-ray micro-computed tomography (microCT), which has been shown to provide a reliable, noninvasive method of constructing VCs (Brodersen *et al.*, 2013; Choat *et al.*, 2015; Knipfer *et al.*, 2015; Bouche *et al.*, 2016). X-ray microCT provides an exciting new opportunity to make parallel observations of embolism spread between tissues, while avoiding potential artefacts associated with many traditional methods of tissue excision before embolism quantification (Choat *et al.*, 2015; Cochard *et al.*, 2015). MicroCT has recently been applied to leaves of conifers (Bouche *et al.*, 2016) and angiosperms (Scoffoni *et al.*, 2017), providing high-resolution spatial detail of the position of embolisms in the xylem. The limitation of this technique is that the temporal sequence of embolism spread is poor, due to the nature of the beam-line protocols, and the potential damage caused by multiple scans of single target organs (McElrone *et al.*, 2013). A newly developed method, the optical VC (OV) technique, provides opportunities for measuring the formation and spread of embolism in xylem within intact leaves (Brodrigg *et al.*, 2016a,b). A significant advantage of the OV technique is that it permits continuous observation over a wide area allowing spatial and temporal details of embolism to be recorded.

In the study presented here we employ a combination of these new techniques, verified by traditional hydraulic methods, thus giving us new insights into critical questions about the spread of embolism throughout tomato (*Solanum lycopersicum*), a common herbaceous and important global crop species. Specifically, we asked: what is the temporal sequence of embolism formation within root, stem and leaf xylem in tomato? Is there any evidence for divergence in vulnerability among tissues?

Materials and Methods

Species and growing conditions

We grew individuals of *S. lycopersicum* L. (var. Rhineland's Rhun) in glasshouse facilities at the University of Tasmania. All seedlings were grown in potting mix (medium 8 : 2 : 1 mix of composted pine bark, coarse river sand, and peat moss) under controlled glasshouse conditions of 23°C : 15°C, day:night temperatures and 16-h photoperiod, with natural light supplemented by sodium vapour lamps to ensure a minimum 300 $\mu\text{mol quanta m}^{-2} \text{s}^{-1}$ at the pot surface. Relative humidity was maintained at *c.* 60% by a

dehumidifier with integrated humidity sensors (ADH-1000, Airrex portable dehumidifier; Hephzibah Co. Ltd, Incheon, South Korea). Before X-ray and optical scanning, plants were removed from the pots and their roots were gently rinsed to remove the loose sand and pine bark mixture. As we observed little embolism within well-hydrated plants (see Results of the microCT analysis) we were confident that this procedure did not damage the roots and introduce artefactual air-entry into the plants.

Individuals were also harvested at two different ages (30 d and 69 d after sowing) to assess proportional biomass allocation. For each age cohort, the plant tissue of three individuals was divided into stems, leaves and roots and was oven-dried for 2 d at 75°C. Material from each individual was subsequently weighed (± 0.001 g; MS204S; Mettler-Toledo, Greifensee, Switzerland) and biomass allocation was expressed as a proportion of total plant weight.

X-ray micro-computed tomography (microCT)

Embolism was visualized in intact stems and roots of tomato plants using synchrotron based X-ray tomography (McElrone *et al.*, 2013). We did not capture microCT images for tomato leaves, largely because of the complex plumbing of the venation network (different vein orders have different vulnerabilities), the fact that only large veins could potentially be resolved and due to severe time considerations at the facility.

Ten seedlings, *c.* 30 cm in height and 60 d old, were transported from the glasshouse facilities at the University of Tasmania to the Australian Synchrotron in Melbourne in moist paper towel and plastic bags. Once at the Imaging and Medical beamline facility each plant was dehydrated to varying water potentials (Ψ_x) by varying their exposure time to air. Leaf water potential was measured on a detached leaf using a Scholander pressure chamber (PMS Instruments, Albany, OR, USA). Initial tests from several leaves from the same individual confirmed that leaf water potential was highly consistent within individuals.

Once each plant was at the desired Ψ_x we mounted it into a fixed position on a stage and scanned it at 30 keV in the synchrotron X-ray beam. The seedlings were rotated continuously through 180° with images collected 0.1° increments yielding 1800 projections. Images were collected with a 2560 × 2160 pixel sCMOS camera (pco.edge 5.5, PCO) at a 150 ms exposure time. The field of view was 14.6 mm × 12.4 mm with a reconstructed image resolution of *c.* 5.9 μm per pixel. Each scan took *c.* 15 min to complete. We scanned both a root section and a stem section of each intact plant by moving the stage up or down. Scans of stems were made *c.* 4 cm above the collar and < 2 cm below the collar for roots. The first two scans (i.e. one each for the stem and root, respectively) detected air-filled vessels caused by embolism events in the intact plant. After these initial scans, we cut the stem below the scanned stem area (within *c.* 1 cm) and scanned the plant two more times, one scan each for the severed stem and root sections. Severing the stem served to create embolisms in all functional xylem conduits allowing functional xylem to be differentiated from nonfunctional or living xylem conduits. Thus, the repeat scans allowed us to compare embolism of intact roots and stems with the fully cavitated state and to generate VCs (see later). We

further verified that the fully-embolized sections were in fact ‘fully embolized’ by comparing the images to cross-sections taken from the same point on the plant (see later).

Since each plant was used to generate a single point on the VC, we were able to exclude the possibility of increasing damage by the X-ray dose impacting the VCs. Immediately following the final (i.e. fourth) scan for each individual plant, a leaf was removed and leaf water potential was measured using a Scholander pressure chamber (PMS Instruments). Again, initial tests from several leaves from the same individual confirmed that leaf water potential was highly consistent within individuals.

The acquired longitudinal images were reconstructed into a ‘stack’ of 2098 transverse TIF images using the XLI CT Workflow application (Commonwealth Scientific and Industrial Research Organization). Three dimensional reconstructions of embolized vessels were generated with AVIZO 9.1 software (FEI Company, Hillsboro, OR, USA) accessed on the MASSIVE visualization environment. By comparing the fully embolized state (i.e. the scan images produced after the plants were cut) with the intact state (i.e. the scan images of the intact tissues) we were able to estimate a proxy for percentage loss of conductivity (PLC) and thus to reconstruct xylem VCs for both roots and stems.

Reconstructing VCs using X-ray images and cross-sections

We cross-sectioned the scanned sections of the roots and stems in the region of the scan using a sliding microtome (Leica Microsystems, North Ryde, Australia) and a BFS-3MP Freezing Stage (Physitemp Instruments, Clifton, NJ, USA). Cross-sections were stained with 5% aqueous toluidine blue solution for *c.* 30 s and photographed on a Leica DM1000 microscope (Leica Microsystems) with a Nikon DS-Fi2 microscope camera (Nikon Instruments, Tokyo, Japan).

Cross-sections were matched up with X-ray micrographs and functional and embolized vessels were identified in cross-sections. There was generally very good agreement between the X-ray micrograph images and the cross-section images and there was no evidence of any large vessels visible with the cross-sections that were not embolized by cutting in the microCT images. Images of the cross-sections also allowed us to differentiate between xylem and pith and to identify individual vessels.

After initial comparison of the X-ray micrographs and the cross-section images, we decided to use the light microscope cross-sections rather than the original micrographs to determine vessel diameters because the resolution of the X-ray CT was not sufficient to distinguish whether voids represented single or pairs of conduits in all cases. Particle analysis in IMAGEJ was used to determine the diameter of each vessel and these data were used to calculate an estimate of the total conductance of each cross-section, k , using Poiseuille's equation:

$$k = \sum (\pi d^4 / 128 \eta), \quad \text{Eqn 1}$$

where d is the vessel diameter, η is the viscosity of water. Maximum k (k_{\max}) for each individual root and stem was

quantified using the image of the fully embolized (i.e. severed) root and stem sections. Native k (k_{native}) of each individual root and stem was obtained from the image of the intact root and stem by subtracting k of any embolized vessels ($k_{\text{embolized vessels}}$) from k_{\max} :

$$k_{\text{native}} = k_{\max} - k_{\text{embolized vessels}} \quad \text{Eqn 2}$$

Although Poiseuille's equation is based on flow through a series of pipes and may imperfectly capture conductance through complex vein networks, we were interested more in capturing *changes* in conductance, rather than absolute measures and thus consider k to be a reasonable proxy for our purposes. Furthermore, there was no evidence for the presence of tyloses or gels within the veins, which may further affect the reliability of the estimate of conductance. In light of this, we quantified an estimate of the PLC by comparing k_{\max} with k_{native} according to the following equation:

$$\text{PLC} = (k_{\max} - k_{\text{native}}) / k_{\max} \cdot 100 \quad \text{Eqn 3}$$

We then fitted a sigmoidal model to the relationship between PLC and leaf Ψ_x :

$$\text{PLC} = 100 / (1 + e^{a(\Psi - b)}) \quad \text{Eqn 4}$$

where b is P_{50} and a is a fitted parameter related to the slope of the curve. Thus, 95% confidence intervals for the PLC data of stems and roots were calculated using bootstrapped values from 2000 simulations conducted in R (R Core Team, 2014).

Optical vulnerability method

Three tomato leaves from three different individuals were set up on a slide scanner (V800 Epson) while remaining attached to the parent plant; roots exposed to enhance drying. Leaves were kept in place using transparent adhesive tape and images of the desiccating leaves were recorded every minute.

A psychrometer (ICT International, Armidale, NSW, Australia) was connected to the petiole of an adjacent leaf to provide a continuous measure of Ψ_x during drying. Periodically, we also measured Ψ_x of three other adjacent leaves using a Scholander pressure chamber (PMS Instruments) to verify the psychrometer readings. We found that after stomatal closure, the rate of decline of Ψ_x was highly linear, there was good agreement between the psychrometer values and those obtained with the pressure chamber, and the pressure chamber readings were highly similar (Supporting Information Fig. S1). Thus we are confident that we were able to accurately quantify the Ψ_x of the target leaves.

Analysis of the image sequences captured during dehydration was done using an image subtraction method in IMAGEJ v.1.47 (National Institutes of Health, Bethesda, MD, USA) (see Brodribb *et al.* (2016a,b) for a more detailed account of image analysis methodology). The image subtraction method highlights rapid changes in light transmission caused by xylem cavitation, while filtering all other slow movement associated with drying. A new

image stack consisting of subtracted images was then thresholded to highlight the embolism events. After thresholding the ‘analyse particles’ function of IMAGEJ was used to isolate embolized vessels by filtering out noise.

Leaf venation, which is composed of multiple vessels, was separated into three vein orders: midrib, secondary (large veins emerging from the midrib) and tertiary (all remaining veins) venation. Regions of interest corresponding to each vein order were created and the ‘Measure Stack’ function was used to measure the number of cavitated pixels in each image for each vein order throughout the image stack. The count of embolized pixels was then summed to give the cumulative number of pixels present in each vein order over time. The product is a temporally and spatially resolved data set indicating the accumulation of embolisms in vein orders. The abrupt start and end of embolization during desiccation enabled the dynamic spread of embolism to be expressed as a percentage of a maximum embolized state in each vein order at each time point. By converting time into Ψ_x we were able to produce an optical VC for each leaf and for the different vein orders within each leaf.

We calculated a proxy for PLC in the whole leaf and within each vein order using Eqn 3, by equating the total number of pixels in the leaf or each vein order that changed from unembolized to embolized to k_{\max} and the sum of embolized veins (i.e. pixels) at each particular Ψ_x to $k_{\text{embolized vessels}}$. We then modelled the VC and extracted relevant parameters for the leaf and vein orders using Eqn 4.

Rehydration kinetic (RK) method

Three plants were dehydrated by withholding water for a period of about a week. At various stages of dehydration, we bagged leaves for at least an hour, allowing them to equilibrate, and subsequently removed a leaflet and measured initial Ψ_x using a Scholander pressure chamber (PMS Instruments). Leaf hydraulic conductance (k_{leaf}) was determined on either the same leaf (if water potential was measured on a leaflet) or a neighbouring leaf by measuring dynamic flow during leaf rehydration (Brodribb & Cochard, 2009). The leaves – which were still attached to the plant at this stage – were cut under water and immediately connected to a flow meter consisting of a capillary tube with known conductance (k_{tube} in $\text{mmol s}^{-1} \text{MPa}^{-1}$) and a pressure transducer (Omega Engineering, Stamford, CT, USA) (Melcher *et al.*, 2012). The hydraulic flux, F (in $\text{mmol m}^{-2} \text{s}^{-1}$), into the leaf was monitored immediately (for the ‘initial’ value) and after 30 s (for a ‘final’ value), at which stage the leaf was removed and Ψ_x was determined after equilibrating for 10–15 min. Leaves were scanned and analysed using IMAGEJ for leaf area (in cm^2). Since the pressure transducer can be read initially (as soon as the leaf is connected) and at the end (immediately before disconnecting the leaf), the method allows two values of k_{leaf} (in $\text{mmol m}^{-2} \text{s}^{-1} \text{MPa}^{-1}$) to be calculated using the following equation:

$$k_{\text{leaf}} = F / \Delta\Psi_x, \quad \text{Eqn 5}$$

where $\Delta\Psi_x$ is the hydraulic driving force and equal to Ψ_x (note: this is the reason for two water potential readings, an ‘initial’ and a ‘final’). The initial and final values of k_{leaf} were compared against

each other and were discarded if variation exceeded *c.* 30%. Values of k_{leaf} (initial) were plotted against initial Ψ_x and fitted with a sigmoidal relationship, from which we were able to extract relevant parameters:

$$k_{\text{leaf}} = k_{\max} / (1 + e^{a(\Psi-b)}) \quad \text{Eqn 6}$$

where k_{\max} was defined as the mean k_{leaf} above -0.5 MPa.

Stomatal closure

In accordance with the cohesion-tension theory, the more distal tissues of a transpiring plant (e.g. leaves) must have lower Ψ_x than more proximal tissues (e.g. roots and stems). However, stomatal closure would have the effect of largely collapsing the water potential gradient within the plant. We investigated the water potential associated with stomatal closure to determine whether there may have existed any gradient in the plant at times when we measured embolism.

Midday stomatal conductance, g_s , of three tomato individuals growing in the glasshouse facilities at the University of Tasmania, was measured using a Li-Cor 6400 (Li-Cor BioSciences, Lincoln, NE, USA). Light intensity in the Li-Cor cuvette was set at $1500 \mu\text{mol m}^{-2} \text{s}^{-1}$, temperature was set to 22°C and relative humidity was maintained at ambient. Fully expanded, sunlit leaves were placed in the chamber for *c.* 20 min before the measurements were recorded to ensure that we captured maximum g_s . Immediately afterwards, leaves were removed from the plant, wrapped in moist tissue paper, bagged, and transported to the laboratory where leaf Ψ_x was measured using a Scholander pressure chamber. The relationship between g_s and leaf Ψ_x was found to fit a sigmoidal model:

$$g_s = g_{s \max} / (1 + e^{a(\Psi-b)}) \quad \text{Eqn 7}$$

where b is the leaf Ψ_x at 50% of maximum g_s ($g_{s \max}$) and a is a fitted parameter related to the slope of the curve. From the modelled relationship we could extract the point of stomatal closure.

Results

MicroCT

We were able to visualize the presence of embolized veins within both roots and stems of intact tomato plants using images obtained by microCT. Three-dimensional rendering of roots showed that embolism occurred in both the adventitious roots and the main root axis (Fig. 1a,b). Using reference scans of the roots or stems after cutting in air we were able to identify all of the functional vessels (Fig. 1c).

As the tomato plants dehydrated (i.e. water potential declined), the number of embolized vessels increased in both stems (compare number of embolized vessels in Fig. 2a and b) and roots (compare number of embolized vessels in Fig. 2c and d). By comparing the images from the fully embolized state with the images of the intact state, we evaluated which vessels had lost functionality as a result of embolism (see insets Fig. 2), which

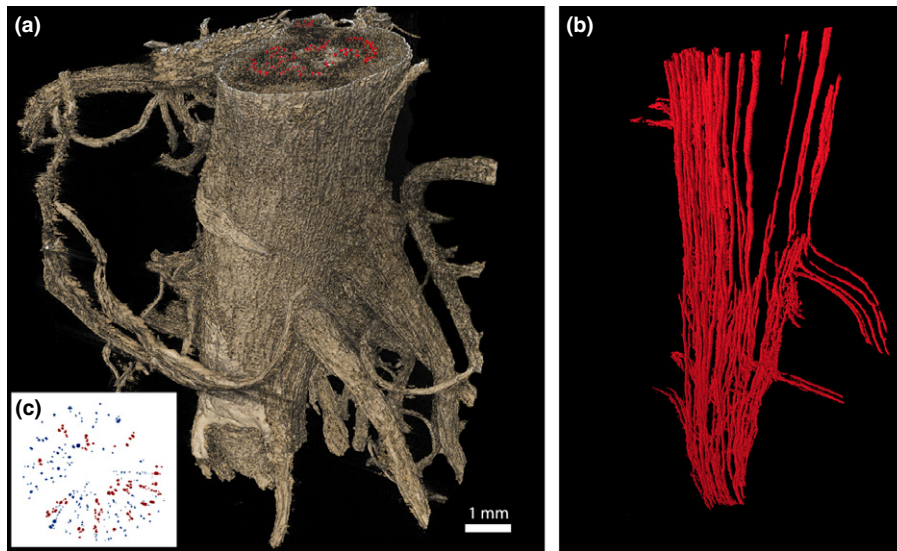


Fig. 1 Three-dimensional (3D) rendering of X-ray micro-computed tomography (microCT) scan images permits visualization of embolism within intact tomato roots. Here we show a 3D rendering of an intact root desiccated to -1.5 MPa (a), illustrating embolized vessels in red (a, b). The 3D images are composed of a 'stack' of two-dimensional (2D) transverse images (see Fig. 2). The inset is a 2D cross-sectional slice of the same root at the same water potential (c), showing only the embolized (red) and nonembolized (blue) vessels. The nonembolized vessels shown in (c) (i.e. the blue vessels) were visible only once the plant had been severed and scanned a second time. Thus (c) is a composite image of two cross-sectional 2D images, one each before and after the plant was severed. From (c) we calculated that the root experienced 49% loss of conductance (see the Materials and Methods section).

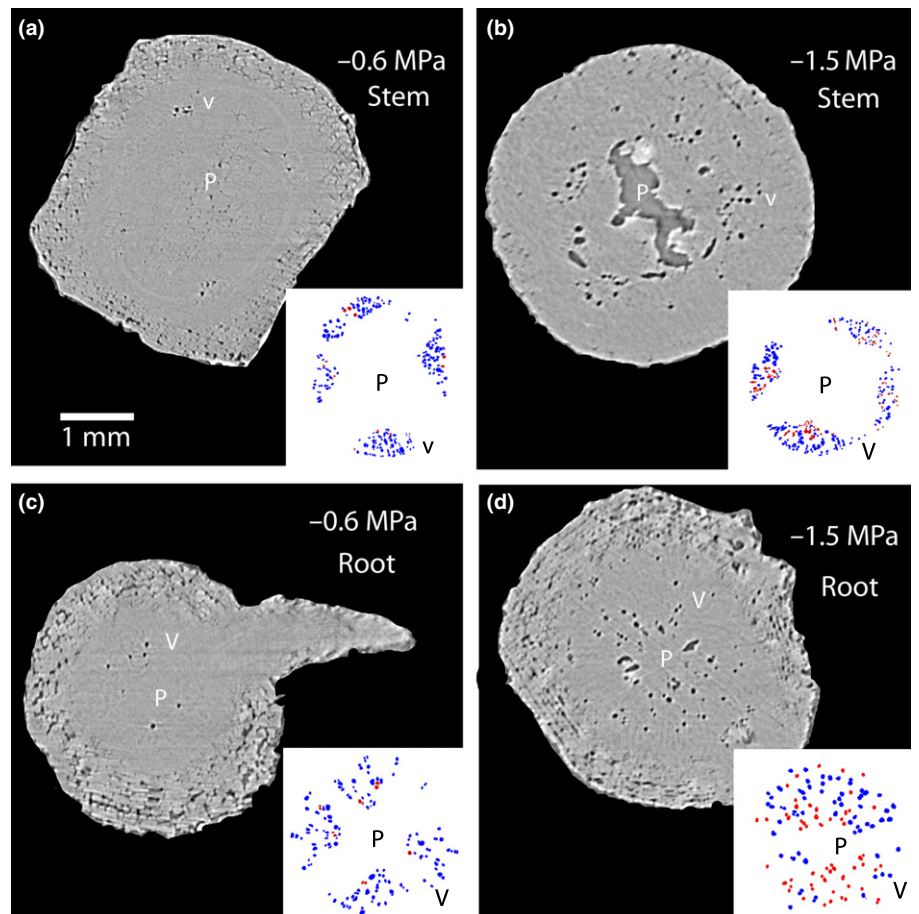


Fig. 2 Two-dimensional (2D) cross-sectional images of stems (a, b) and roots (c, d) of tomato at two different water potentials obtained using the X-ray micro-computed tomography (microCT) indicate that plants at different water potentials experienced different levels of embolism. Here we show a comparison of embolism formation within vessels of plants at -0.6 MPa (a, c) and -1.5 MPa (b, d). The insets show vessels that were embolized in the intact plant (in red) and those that were embolized after the plant had been cut (in blue). By comparing the fully embolized state to the intact state we were able to gain a proxy for percentage loss of conductance (see the Materials and Methods section). P, pith; V, vessels.

provided the basis for our proxy for PLC and for reconstructing xylem VCs for both roots and stems (Fig. 3a). We found little difference in the incipient air-seeding pressure between intact roots and stems (Fig. 3a: Table 1). Due to time constraints at the Imaging and Medical beamline facility we were only able to dehydrate tomato plants to leaf Ψ_x values of -1.6 MPa. At this leaf Ψ_x we observed *c.* 40% embolism in stems and roots imaged by X-ray microCT, thus we used P_{40} (leaf Ψ_x at 40% loss of conductance) as a reference point for comparison between tissues and methods. Although P_{40} was 0.2 MPa lower in intact stems compared with intact roots there was substantial overlap in the 95% confidence intervals for both curves over the range of measured Ψ_x (Fig. 3a: Table 1).

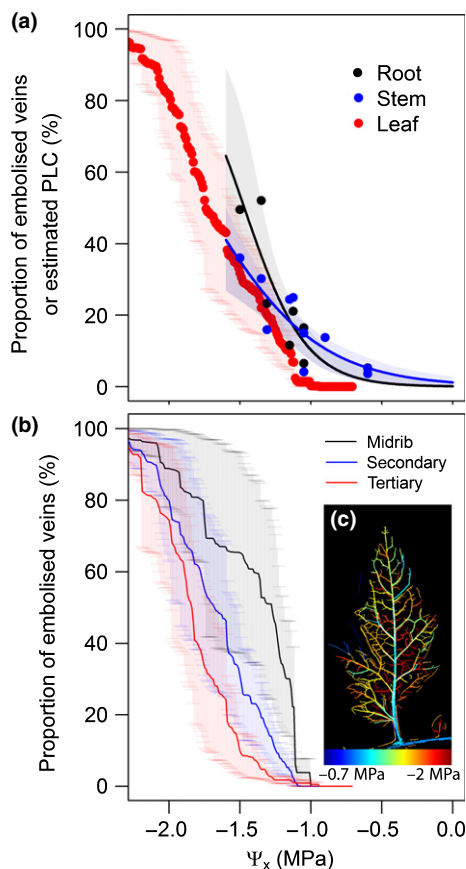


Fig. 3 Xylem vulnerability curve (VC) for roots, stems [obtained from X-ray micro-computed tomography (microCT) scan images] and leaves (generated by the optical vulnerability technique) of tomato (a) showing little difference between the three tissue types. Shaded bands are 95% confidence intervals and bars are standard errors. For the microCT data each data point for roots and stems represents a different individual. Within the leaves (b, c) there was some differentiation in the water potential (Ψ_x) at which different vein orders embolized. The larger diameter veins (i.e. midrib) tended to embolize at higher water potential, followed by secondary veins and then tertiary veins. The inset shows the water potential at which each different vein became embolized. Colours indicate the water potential that each vein or vessel was at when embolism was first observed, with cooler colours (e.g. blue/turquoise) being less negative water potentials and warmer (e.g. red/maroon) being more negative water potentials. Error bars on the VCs are standard errors ($n = 3$).

Optical vulnerability method

Xylem embolism within leaves of tomato was observable using the OV method recently described by Brodribb *et al.* (2016b). Based on the accumulation of leaf vein embolisms we were able to estimate the proportion of embolized vascular tissue (which we used as a proxy for PLC) and thus to reconstruct the xylem VC of tomato leaves (Fig. 3a). As the tomato plants dehydrated, the number of embolized veins within the leaf increased, following a sigmoidal function (Fig. 3a). The P_c and P_{40} values obtained from the leaf using the OV method were similar to those values obtained for the stems with the microCT scans (Fig. 3a; Table 1).

Using the OV method we were also able to capture variation in embolism propagation within the leaf vein network (Fig. 3b,c). The midrib in tomato leaves was more vulnerable than the secondary and tertiary veins and the tertiary veins were consistently less vulnerable than either the midrib or the secondary veins (Fig. 3b,c; Table 1).

Rehydration kinetic (RK) method

We observed a sigmoidal relationship between k_{leaf} and leaf Ψ_x in tomato leaves using the rehydration kinetic (RK) method (Fig. 4a). At leaf Ψ_x higher than P_c , k_{leaf} remained relatively constant at k_{max} , but thereafter k_{leaf} declined rapidly (Fig. 4a). Initial loss of k_{leaf} (measured hydraulically) occurred at the same water potential as the start of embolism, as observed using the OV technique (Table 1). Thereafter, the two curves began to diverge slightly, with declines in k_{leaf} measured with the RK method preceding those observed with the OV method (Table 1). Critical water potential values measured with the RK method were intermediate between those in the midrib and secondary veins observed using the OV method (Table 1). There was no difference in P_{40} between the leaves recorded by the RK method and the roots and stems observed using microCT (Table 1).

Stomatal conductance

Mean maximum g_s in tomato plants was 131.2 ± 15.8 $\text{mmol m}^{-2} \text{s}^{-1}$. After withholding water, tomato stomata started to close at leaf Ψ_x below -0.65 MPa and were fully closed (g_s reaching a stable minimum) at -0.98 ± 0.02 MPa (Fig. 4b).

Discussion

The ability to monitor embolism within intact roots, stems and leaves provides tremendous opportunity to resolve crucial questions surrounding embolism formation and spread within a plant (Cochard *et al.*, 2013). Through a combination of techniques that allowed us to visualize the spread of embolism within intact roots, stems and leaves of tomato plants we showed that there is little variation in xylem resistance to embolism between these tissues. A lack of hydraulic segmentation among tissues of tomato contrasts with previous data from woody plants (Alder *et al.*, 1996). One potential explanation for this lack of vulnerability-differentiation in tomato, that

Table 1 A comparison of critical water potential values associated with varying impacts of embolism on hydraulic conductance for different tissues and leaf vein orders of tomato observed using three different techniques

Technique	Tissue	P_e	Water potential (MPa) \pm SE		
			P_{40}	P_{50}	P_{88}
microCT	Root	-1.04	-1.38 \pm 0.05 ^{ab}	—	—
	Stem	-0.95	-1.58 \pm 0.21 ^{abcd}	—	—
Optical vulnerability	Leaf	-1.24 \pm 0.01 ^b	-1.59 \pm 0.01 ^c	-1.68 \pm 0.01 ^c	-2.13 \pm 0.01 ^b
	Midrib	-0.97 \pm 0.01 ^a	-1.31 \pm 0.01 ^a	-1.41 \pm 0.01 ^a	-1.86 \pm 0.01 ^a
	Secondary veins	-1.27 \pm 0.01 ^b	-1.60 \pm 0.01 ^c	-1.69 \pm 0.01 ^c	-2.11 \pm 0.21 ^{abc}
	Tertiary veins	-1.51 \pm 0.01 ^c	-1.77 \pm 0.01 ^d	-1.84 \pm 0.01 ^d	-2.18 \pm 0.01 ^c
Rehydration kinetics	Leaf	-1.28 \pm 0.09 ^{abc}	-1.49 \pm 0.01 ^b	-1.54 \pm 0.01 ^b	-1.8 \pm 0.09 ^{abc}

Note: P_e is the air-entry water potential, P_{40} , P_{50} , P_{88} are the water potential associated with 40%, 50% and 88% loss of hydraulic conductance, respectively. Values are mean \pm standard error (SE) and superscript letters denote results from statistical tests conducted between tissue types. Differences were deemed significant at $p < 0.05$.

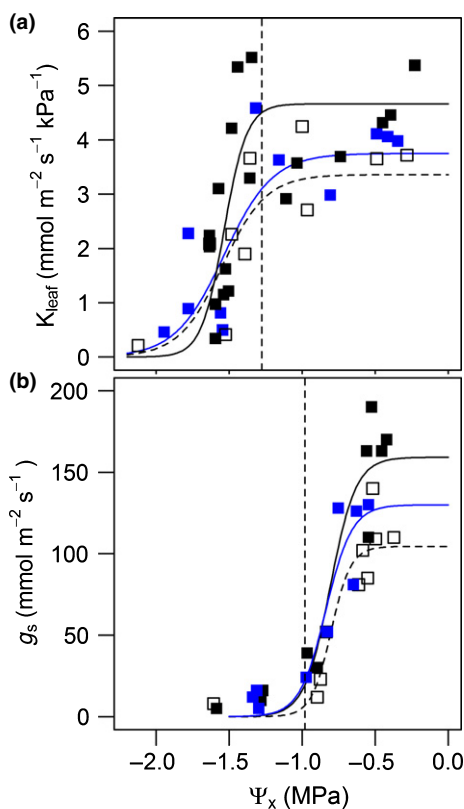


Fig. 4 Leaf hydraulic conductance (K_{leaf} , obtained with the rehydration kinetic (RK) method) (a) initially remained relatively constant in tomato leaves, but declined rapidly once leaf xylem water potential (Ψ_x) fell below -1.28 MPa (i.e. the air-entry water potential, P_e , indicated by the vertical dashed line). The relationship between stomatal conductance (g_s) and Ψ_x (b) indicated that stomatal closure (indicated by the vertical dashed line) occurred at a higher leaf water potential than incipient embolism formation. The different colours indicate individual plants.

is consistent with the HSH, is that tomato proportions biomass relatively evenly among tissues (Fig. S2). A lack of hydraulic priority might then be expected, as observed here in tomato. Poorter *et al.* (2012) report substantial variation in leaf, stem and root mass fractions within herbaceous species, particularly

between monocots and eudicots, and we might therefore predict substantial variation in the extent of divergence of xylem vulnerability among tissues within species of this functional type. Our findings suggest that further studies should address the generality of hydraulic segmentation among tissues of other herbaceous species and under-represented species.

Although we found scarce evidence for differentiation of xylem vulnerability among tissues at the scale of whole plant, within a leaf the midrib embolized at higher Ψ_x than lower order veins. This finding appears to be general among leaves for those species that have been sampled (Brodribb *et al.*, 2016a,b) and might be important for maintaining homogeneous supply of water to leaf mesophyll tissues as the plant dehydrates (Scoffoni *et al.*, 2017). Slight differences in leaf water potentials associated with 40% and 50% declines in k_{leaf} recorded with the RK and the OV methods, coupled with variation of embolism formation among the different vein orders, allowed us to investigate which vein orders are most important for water transport within leaves. Declines in k_{leaf} were intermediate between observed embolism in the midrib and secondary vein orders, and not closely associated with embolism in the tertiary veins. These results suggest a degree of functional redundancy within the midrib. Despite this possibility, the magnitude of hydraulic conductance in the minor veins at low leaf water potentials is likely to be relatively low, as suggested by our k_{leaf} measurements, which showed almost negligible k_{leaf} at leaf water potentials < -1.75 MPa.

Scaling of vulnerability within the vein network was not observed in the root system, where we found that adventitious roots embolized simultaneously with vessels in the main root axis and that embolism events were in fact continuous between these two tissues (Fig. 1b). However, we cannot rule out the possibility of differences in vulnerability within the root system, as we were unable to visualize embolism within very fine roots, which may provide a better analogue for the lower order veins. Recent work on a woody species suggests that declines in root hydraulic conductance are linked to the formation of cortical lacunae in fine roots (Cuneo *et al.*, 2016).

Signs of permanent leaf damage in tomato leaves were observed at Ψ_x below -1.9 MPa and became more pronounced until leaf Ψ_x of -2.9 MPa (Fig. S3) at which point we were unable to reliably

measure Ψ_x . Thus, our results indicate that incipient embolism is associated with severe, but nonlethal water stress in tomato and that substantial loss of k_{leaf} and extensive embolism is associated with permanent leaf damage. The amount of damaged tissue appeared to increase at leaf Ψ_x lower than P_{88} in leaves, consistent with the notion that points of death and recovery in angiosperms can be defined from P_{95} in leaves (Brodrribb & Cochard, 2009).

A potential limitation of the current work is that we used multiple techniques to assess propagation of embolism within individual plants. Although current X-ray microCT techniques permit visualization of embolism within small, soft tissues such as petioles, the damaging nature of X-rays imposes severe limitations on the ability to scan an individual multiple times to resolve the temporal detail of embolism propagation (Scoffoni *et al.*, 2017).

Also, we assumed that leaf water potential was in equilibrium with root and stem water potential following stomatal closure based on the notion that stomatal closure would largely collapse the water potential gradient within the plant due to lack of transpiration. Although stomatal closure occurred some 12 h before initial embolism events (thus providing adequate time for equilibration within the plant), very low rates of cuticular water loss or loss of water through leaky stomata could have maintained very small gradients within the plant. Although we saw no disagreement between leaf and stem water potentials measured on plants with closed stomata (unpublished data), it is possible that severe cavitation may lead to gradients developing at the end of the cavitation cycle. Understanding the distribution of water potential within severely water-stressed plants is complicated by technical limitations of the Scholander technique (Tyree & Hammel, 1972; Turner, 1981) and this is a future direction of study that will permit us to further resolve questions of embolism propagation among tissues. Doing so in herbaceous species is particularly important since many herbaceous angiosperms, like tomato, are important agricultural crop species.

Acknowledgements

The authors thank the technical staff at the Australian Synchrotron Imaging and Medical Beamline in Melbourne for assisting with the micro-computed tomography methodology. Jennifer Peters, Danielle Creek and Rosana Lopez are thanked for assistance with measurements at the Australian Synchrotron. R.P.S. received a postdoctoral abroad scholarship from the South African National Research Foundation (Grant 88290). R.P.S., B.C. and T.J.B. received a visitor's scholarship from the Australian Synchrotron, which partially paid for the visit to the facility. B.C. was supported by an Australian Research Council Future Fellowship (FT130101115). The authors thank several anonymous reviewers for suggestions on improvements to the manuscript.

Author contributions

T.J.B., B.C. and R.P.S. designed and performed the research. R.P.S. and T.J.B. performed the data analysis. R.P.S. wrote the manuscript with input from T.J.B. and B.C.

References

- Alder NN, Sperry JS, Pockman WT. 1996. Root and stem xylem embolism, stomatal conductance, and leaf turgor in *Acer grandidentatum* populations along a soil moisture gradient. *Oecologia* 105: 293–301.
- Bouche PS, Delzon S, Choat B, Badel E, Brodrribb TJ, Burtlett R, Cochard H, Charra-Vaskou K, Lavigne B, Li S *et al.* 2016. Are needles of *Pinus pinaster* more vulnerable to xylem embolism than branches? New insights from X-ray computed tomography. *Plant, Cell & Environment* 39: 860–870.
- Brodersen CR, McElrone AJ, Choat B, Lee EF, Shackel KA, Matthews MA. 2013. *In vivo* visualizations of drought-induced embolism spread in *Vitis vinifera*. *Plant Physiology* 161: 1820–1829.
- Brodrribb TJ, Bienaimé D, Marmottant P. 2016a. Revealing catastrophic failure of leaf networks under stress. *Proceedings of the National Academy of Sciences, USA* 113: 4865–4869.
- Brodrribb TJ, Cochard H. 2009. Hydraulic failure defines the recovery and point of death in water-stressed conifers. *Plant Physiology* 149: 575–584.
- Brodrribb T, Hill RS. 1999. The importance of xylem constraints in the distribution of conifer species. *New Phytologist* 143: 365–372.
- Brodrribb TJ, McAdam SAM, Jordan GJ, Martins SCV. 2014. Conifer species adapt to low-rainfall climates by following one of two divergent pathways. *Proceedings of the National Academy of Sciences, USA* 111: 14489–14493.
- Brodrribb TJ, Skelton RP, McAdam SAM, Bienaimé D, Lucani CJ, Marmottant P. 2016b. Visual quantification of embolism reveals leaf vulnerability to hydraulic failure. *New Phytologist* 209: 1403–1409.
- Bucci SJ, Scholz FG, Campanello PI, Montti L, Jimenez-Castillo M, Rockwell FA, La Manna L, Guerra P, Bernal PL, Troncoso O *et al.* 2012. Hydraulic differences along the water transport system of South American *Nothofagus* species: do leaves protect the stem functionality? *Tree Physiology* 32: 880–893.
- Challinor AJ, Ewert F, Arnold S, Simelton E, Fraser E. 2009. Crops and climate change: progress, trends, and challenges in simulating impacts and informing adaptation. *Journal of Experimental Botany* 60: 2775–2789.
- Choat B. 2013. Predicting thresholds of drought-induced mortality in woody plant species. *Tree Physiology* 33: 669–671.
- Choat B, Badel E, Burtlett R, Delzon S, Cochard H, Jansen S. 2015. Non-invasive measurement of vulnerability to drought induced embolism by X-ray microtomography. *Plant Physiology* 170: 273–282.
- Choat B, Jansen S, Brodrribb TJ, Cochard H, Delzon S, Bhaskar R, Bucci SJ, Feild TS, Gleason SM, Hacke UG *et al.* 2012. Global convergence in the vulnerability of forests to drought. *Nature* 491: 752–755.
- Choat B, Lahr EC, Melcher PJ, Zwieniecki MA, Holbrook NM. 2005. The spatial pattern of air seeding thresholds in mature sugar maple trees. *Plant, Cell & Environment* 28: 1082–1089.
- Cochard H, Badel E, Herbette S, Delzon S, Choat B, Jansen S. 2013. Methods for measuring plant vulnerability to cavitation: a critical review. *Journal of Experimental Botany* 64: 4779–4791.
- Cochard H, Cruiziat P, Tyree MT. 1992. Use of positive pressures to establish vulnerability curves. *Plant Physiology* 100: 205–209.
- Cochard H, Delzon S, Badel E. 2015. X-ray microtomography (micro-CT): a reference technology for high-resolution quantification of xylem embolism in trees. *Plant, Cell & Environment* 38: 201–206.
- Cuneo I, Knipfer T, Brodersen C, McElrone AJ. 2016. Mechanical failure of fine root cortical cells initiates plant hydraulic decline during drought. *Plant Physiology* 172: 1669–1678.
- Froux F, Ducrey M, Dreyer E, Huc R. 2004. Vulnerability to embolism differs in roots and shoots and among three Mediterranean conifers: consequences for stomatal regulation of water loss? *Trees* 19: 137–144.
- Jinagool W, Rattanawong R, Sangsing K, Barigah TS, Gay F, Cochard H, Kasemsap P, Herbette S. 2015. Clonal variability for vulnerability to cavitation and other drought-related traits in *Hevea brasiliensis* Müll. Arg. *Journal of Plant Hydraulics* 2: e001.
- Johnson DM, McCulloh KA, Meinzer FC, Woodruff DR, Eissenstat DM. 2011. Hydraulic patterns and safety margins, from stem to stomata, in three eastern U.S. tree species. *Tree Physiology* 31: 659–668.
- Kavanagh KL, Bond BJ, Aitken SN, Gartner BL, Knowe S. 1999. Shoot and root vulnerability to xylem cavitation in four populations of Douglas-fir seedlings. *Tree Physiology* 19: 31–37.

- Knipfer T, Brodersen CR, Zedan A, Kluepfel DA, McElrone AJ. 2015. Patterns of drought-induced embolism formation and spread in living walnut saplings visualized using X-ray microtomography. *Tree Physiology* 35: 744–755.
- McCulloh KA, Johnson DM, Petitmermet J, McNellis B, Meinzer FC, Lachenbruch B. 2015. A comparison of hydraulic architecture in three similarly sized woody species differing in their maximum potential height. *Tree Physiology* 35: 723–731.
- McElrone AJ, Choat B, Parkinson DY, MacDowell AA, Brodersen CR. 2013. Using high resolution computed tomography to visualize the three dimensional structure and function of plant vasculature. *Journal of Visualized Experiments* 74: e50162–e50173.
- Melcher PJ, Michele Holbrook N, Burns MJ, Zwieniecki MA, Cobb AR, Brodribb TJ, Choat B, Sack L. 2012. Measurements of stem xylem hydraulic conductivity in the laboratory and field. *Methods in Ecology and Evolution* 3: 685–694.
- Ogasa M, Miki NH, Murakami Y, Yoshikawa K. 2013. Recovery performance in xylem hydraulic conductivity is correlated with cavitation resistance for temperate deciduous tree species. *Tree Physiology* 33: 335–344.
- Poorter H, Niklas KJ, Reich PB, Oleksyn J, Poot P, Mommer L. 2012. Biomass allocation to leaves, stems and roots: meta-analyses of interspecific variation and environmental control. *New Phytologist* 193: 30–50.
- R Core Team. 2014. *R language definition v.3.1.1*. [WWW document] URL <https://www.r-project.org/> [accessed November 2015].
- Scoffoni C, Albuquerque C, Brodersen CR, Townes SV, John GP, Cochard H, Buckley TN, McElrone AJ, Sack L. 2017. Leaf vein xylem conduit diameter influences susceptibility to embolism and hydraulic decline. *New Phytologist* 213: 1076–1092.
- Sperry JS, Ikeda T. 1997. Xylem cavitation in roots and stems of Douglas-fir and white fir. *Tree Physiology* 17: 275–280.
- Turner NC. 1981. Techniques and experimental approaches for the measurement of plant water status. *Plant and Soil* 58: 339–366.
- Tyree MT, Cochard H, Cruziat P, Sinclair B, Ameglio T. 1993. Drought-induced leaf shedding in walnut: evidence for vulnerability segmentation. *Plant, Cell & Environment* 16: 879–882.
- Tyree MT, Ewers FW. 1991. Tansley review no. 34. The hydraulic architecture of trees and other woody plants. *New Phytologist* 119: 345–360.
- Tyree MT, Hammel HT. 1972. The measurement of the turgor pressure and the water relations of plants by the pressure-bomb technique. *Journal of Experimental Botany* 23: 267–282.
- Tyree MT, Snyderman DA, Wilmot TR, Machado J. 1991. Water relations and hydraulic architecture of a tropical tree (*Schefflera morototoni*). *Plant Physiology* 96: 1105–1113.
- Tyree MT, Sperry JS. 1988. Do woody plants operate near the point of catastrophic xylem dysfunction caused by dynamic water stress? Answers from a model. *Plant Physiology* 88: 574–580.
- Tyree MT, Sperry JS. 1989. Vulnerability of xylem to cavitation and embolism. *Annual Reviews of Plant Physiology & Plant Molecular Biology* 40: 19–38.
- Urli M, Porté AJ, Cochard H, Guengant Y, Burrell R, Delzon S. 2013. Xylem embolism threshold for catastrophic hydraulic failure in angiosperm trees. *Tree Physiology* 33: 672–683.
- Zimmermann MH. 1978. Hydraulic architecture of some diffuse-porous trees. *Canadian Journal of Botany* 56: 2286–2295.
- Zimmermann MH. 1983. *Xylem structure and the ascent of sap*. Berlin, Germany: Springer-Verlag.

Supporting Information

Additional Supporting Information may be found online in the Supporting Information tab for this article:

Fig. S1 Relationship between leaf water potential of tomato assessed with the psychrometer and with the Scholander pressure chamber.

Fig. S2 Biomass allocation in tomato individuals varies with age; younger individuals allocate more to leaves, while older individuals invest more evenly.

Fig. S3 Signs of permanent leaf damage in tomato started to increase once leaf water potential declined below -1.9 MPa.

Please note: Wiley Blackwell are not responsible for the content or functionality of any Supporting Information supplied by the authors. Any queries (other than missing material) should be directed to the *New Phytologist* Central Office.



About New Phytologist

- *New Phytologist* is an electronic (online-only) journal owned by the New Phytologist Trust, a **not-for-profit organization** dedicated to the promotion of plant science, facilitating projects from symposia to free access for our Tansley reviews.
- Regular papers, Letters, Research reviews, Rapid reports and both Modelling/Theory and Methods papers are encouraged. We are committed to rapid processing, from online submission through to publication 'as ready' via *Early View* – our average time to decision is <28 days. There are **no page or colour charges** and a PDF version will be provided for each article.
- The journal is available online at Wiley Online Library. Visit www.newphytologist.com to search the articles and register for table of contents email alerts.
- If you have any questions, do get in touch with Central Office (np-centraloffice@lancaster.ac.uk) or, if it is more convenient, our USA Office (np-usaoffice@lancaster.ac.uk)
- For submission instructions, subscription and all the latest information visit www.newphytologist.com